REPORT DOCUMENTATION PAGE

Form Approved
OMB No. 074-0188

1. AGENCY USE ONLY (Leave blank)	2. REPORT DATE	3. REPORT TYPE AND DATES COVERED
	1994	Technical report, 21-22 March

4. TITLE AND SUBTITLE
Optical Monitoring of the Oxidation of Methane in Supercritical Water

5. FUNDING NUMBERS
N/A

6. AUTHOR(S)
Richard R. Steeper and Steven F. Rice

7. PERFORMING ORGANIZATION NAME(S) AND ADDRESS(ES)
Combustion Research Facility
Sandia National Laboratories
Livermore, CA 94551-0969

8. PERFORMING ORGANIZATION REPORT NUMBER
WSS/CI 94-008

9. SPONSORING / MONITORING AGENCY NAME(S) AND ADDRESS(ES)
SERDP
901 North Stuart St. Suite 303
Arlington, VA 22203

10. SPONSORING / MONITORING AGENCY REPORT NUMBER
N/A

11. SUPPLEMENTARY NOTES
Presented at the 1994 Spring Meeting of the Western States Section/The Combustion Institute, Davis, CA March 21-22, 1994. This work was supported in part by SERDP.

12a. DISTRIBUTION / AVAILABILITY STATEMENT
Approved for public release: distribution is unlimited

12b. DISTRIBUTION CODE
A

13. ABSTRACT ***(Maximum 200 Words)***

Experiments were conducted in a static, high-pressure reactor to investigate the oxidation of methane in supercritical water. Pressures ranged from 138 to 275 bar, temperatures from 380 to 440 ^{0}C, and equivalence ratios from 0.2 to 2.0 for intial methane concentrations around 0.1 mole/1. In these experiments, Raman spectroscopy was used as an *in-situ* diagnostic to monitor the concentrations of methane, oxygen, and carbon dioxide. Over this pressure range the reaction rate of methane with oxygen is unexpectedly observed to decrease with increasing pressure. A non-linear least squares fit was pperformed to determine four global reaction rate parameters. In contrast to results from experiments at lower initial methane concentrations, the reaction order dependency on methane is found here to be greater than unity. This finding implies that the former results cannot safely extrapolate to concentrations around 0.1 mole/1.

14. SUBJECT TERMS
supercritical water, Raman spectroscopy, SERDP

15. NUMBER OF PAGES
20

16. PRICE CODE
N/A

17. SECURITY CLASSIFICATION OF REPORT	18. SECURITY CLASSIFICATION OF THIS PAGE	19. SECURITY CLASSIFICATION OF ABSTRACT	20. LIMITATION OF ABSTRACT
unclass	unclass	unclass	UL

WSS/CI 94-008

Optical Monitoring of the Oxidation of Methane in Supercritical Water

Richard R. Steeper and Steven F. Rice

(Presented at the 1994 Spring Meeting of the
Western States Section/The Combustion Institute
Davis, California, March 21-22, 1994)

Sandia National Laboratories

Optical Monitoring of the Oxidation of Methane in Supercritical Water

Richard R. Steeper and Steven F. Rice

Combustion Research Facility

Sandia National Laboratories

Livermore, California 94551-0969

Abstract

Experiments were conducted in a static, high-pressure reactor to investigate the oxidation of methane in supercritical water. Pressures ranged from 138 to 275 bar, temperatures from 380 to 440 °C, and equivalence ratios from 0.2 to 2.0 for initial methane concentrations around 0.1 mole/l. In these experiments, Raman spectroscopy was used as an *in-situ* diagnostic to monitor the concentrations of methane, oxygen, and carbon dioxide. Over this pressure range the reaction rate of methane with oxygen is unexpectedly observed to decrease with increasing pressure. A non-linear least squares fit was performed to determine four global reaction rate parameters. In contrast to results from experiments at lower initial methane concentrations, the reaction order dependency on methane is found here to be greater than unity. This finding implies that the former results cannot safely extrapolate to concentrations around 0.1 mole/l.

Introduction

Supercritical water oxidation (SCWO) is an emerging technology being developed by many laboratories and industries for the treatment of hazardous wastes. It is appropriate for the destruction of a wide variety of waste streams composed of up to 20% organics in water. Numerous studies have demonstrated that the process achieves destruction and removal efficiencies of 99.99% for residence times from 10 to 30 seconds.[1-3]

The SCWO process involves pressurizing and heating waste and oxidizer streams to conditions above the thermodynamic critical point of water (T_c = 374 °C, P_c = 221 bar). Typical reactor conditions are 250 bar and 450-600 °C. Water at these conditions has a density of about one tenth that of liquid water and behaves for the most part as a dense gas. Most organics, as well as combustion gases such as O_2, CO_2, and N_2, are miscible in all proportions with water at these densities. As a result, the waste and oxidizer mix to form a single-phase fluid in which oxidation reactions proceed without the delays associated with interphase transport. Operating at densities two orders of magnitude greater than atmospheric provides high reaction rates at moderate temperatures. Despite the high density, mass diffusivity remains favorably high—and viscosity low—compared to liquid-phase transport.

The development of this technology depends on understanding the reaction kinetics of a wide variety of compounds at SCWO conditions. Predictive chemistry models, as they become available, will play an important role in finding answers to design problems including: (1) predicting reaction rate dependency on temperature, pressure, and species concentrations; (2) calculating heat release rates and temperature histories during reaction; (3) predicting reaction completeness and byproduct profiles; (4) estimating catalysis effects; and (5) scaling laboratory- and bench-scale experimental results to commercial scale reactors. A long-term goal of our work is the development of detailed elementary mechanisms for the reaction of rate-limiting species such as methane and methanol, with simplified global expressions for the reaction rates serving as near-term design tools.

Several experimental studies in the literature have produced empirical reaction mechanisms for the SCWO of simple hydrocarbons including carbon monoxide,[4] methanol,[5] methane,[6] and phenol.[7] Because these experiments were performed in plug flow reactors, fuel and oxidizer concentrations were limited to low levels attainable in water/gas saturators. For difficult-to-oxidize compounds such as methane, temperatures were necessarily high to provide sufficient destruction at accessible residence times. Samples were extracted from the quenched effluent and analyzed to yield a single data point per experiment. Other researchers have experimented with increasing the data collection rate by using *in-situ* optical measurement techniques.[8] This paper describes methane oxidation experiments performed in a constant volume SCWO reactor. This reactor provides the means to operate at conditions complementary to those characteristic of plug flow experiments and permits the application of laser-based diagnostics to obtain *in-situ* data.

Our experiments were conducted in an optically accessible static reactor permitting the continual measurement of methane, oxygen, nitrogen, and carbon dioxide concentrations via spontaneous Raman spectroscopy. Initial methane concentrations typical of commercial SCWO processes (typically 1 mole%) were used, while temperatures (~ 400 °C) were dictated by the need for an appropriate reaction time scale (10 minutes to several hours). In the experiments, rich to lean equivalence ratios were investigated and total pressure was varied by a factor of two. Our analysis of the data was motivated by three goals: (1) to determine the reaction order with respect to methane concentration, (2) to determine the temperature dependence of the reaction rate, and (3) to determine the pressure dependence of the reaction rate.

Experimental

The externally heated Inconel reactor, illustrated in Figure 1 and described elsewhere,[9] contains a 15-ml combustion chamber accessed by 3 sapphire windows and 5 high-pressure ports. An argon-ion laser (514.5 nm) provides a 1-W probe beam for concentration measurements; the Raman-scattered light is dispersed through a 0.85-m monochromator and detected using an intensified-diode-array detector. A gas-handling system pressurizes small volumes of fuel and oxidizer for delivery to the reactor by way of three high-pressure ports. The fourth port houses a 1/16-inch sheathed Inconel thermocouple inserted into the combustion chamber. The final port houses a pressure transducer.

The first step of a typical experiment is calibration of the Raman diagnostic. The gas to be calibrated (methane, oxygen-nitrogen mixture, or carbon dioxide) is loaded into the preheated reactor and the Raman signal is recorded over a range of total pressures. For methane, we have demonstrated[9] that the integrated intensity of the calibration spectrum is equivalent to that recorded for the same number of moles of methane in a supercritical water mixture. Thus, our calibrations provide the functional relationship between integrated Raman signals collected during our experiments and the corresponding time-resolved concentrations of methane, oxygen, nitrogen, and carbon dioxide. Figure 2 shows a typical Raman spectrum of methane recorded in supercritical water.

Following calibration, the reactor is charged with water to one of two pressure ranges used in these experiments (approximately 138 bar and 275 bar). Reactor temperature is held constant at a value ranging from 380 to 440 °C. When the conditions are stable, a specific amount of methane is injected at constant pressure, and then all exhaust ports are sealed. The total pressure is carefully chosen so that the subsequent constant-volume addition of oxygen will bring final pressure to either 275 bar (high-pressure experiments) or 138 bar (low-pressure experiments). Methane concentration is measured optically at this point to establish initial conditions. A lean , stoichiometric, or rich amount of oxygen is then quickly injected (~15 sec) and the experimental clock is started. We chose a 50 mole% mixture of oxygen and nitrogen for our oxidizer to (1) avoid spontaneous flames associated with injection of pure oxygen[9], and (2) to provide a diagnostic (i.e., the unchanging nitrogen concentration) to monitor stability of the optical measurements.

The remainder of the experiment consists of serially recording methane, oxygen, carbon dioxide, and nitrogen spectra along with time, temperature, and pressure until the methane is depleted. Detector integration times range from 15 seconds for methane to 75 seconds for carbon dioxide, chosen to optimize both signal-to-noise ratio and the time resolution of our measurements.

Results and Discussion

Figure 3 shows two examples of the experimental results at 400 °C under fuel-lean (Fig 3a), and fuel-rich (Fig. 3b) conditions. The plots begin at the first methane and oxygen measurements made following oxygen injection. Figure 4 presents the results for a fuel-lean experiment at 440 °C. The symbols show the evolution of methane, oxygen, and carbon dioxide during supercritical water oxidation. The solid line in the plots is a global fit discussed below. Carbon balance can be obtained by comparing the sum of CH_4 and CO_2 concentrations with the initial methane concentration (recorded before time zero). In Figure 3, CH_4 and CO_2 account for all the carbon of the initial methane concentrations (0.178 mole/l for Figure 3a and 0.327 mole/l for Figure 3b). At the higher temperatures represented by Figure 4 and early in the reaction, the sum of CO_2 and CH_4 does not account for all the carbon (initial methane concentration, 0.158 mole/l). We detected only weak CO signals spectroscopically, and decided not to pursue CO measurement in these experiments. We estimate that the maximum measurement uncertainty for a single methane measurement is 14 % (one standard deviation).

Concentration- and Temperature- Dependence of the Global Methane Reaction Rate

The 15 high-pressure and 11 low-pressure experiments sampled a wide range of pressures, temperatures, initial methane concentrations, and fuel equivalence ratios. Data from the high- and low- pressure series were fitted separately to a one-step global rate expression:

$$d[CH_4]/dt = -k\,[CH_4]^a[O_2]^b, \qquad (1)$$

where $k = A \exp(-E_a/k_BT)$, and $[O_2]$ is related to $[CH_4]$ by the one-step stoichiometry. A Marquardt,[10] non-linear, least-squares routine was used with time taken as the independent variable. Table 1 summarizes the data sets used for the fits: at 275 bar, 219 points from 15 runs were fitted, and at 138 bar, 128 points from 11 runs were used. Table 2 shows the results of the fits. Table 2 also contains the best-fit parameters for methane oxidation obtained by Webley, et. al.[6] for their data at significantly higher temperatures (550°C- 600°C) and lower CH_4 concentrations (~ 1 $x10^{-3}$ moles/l).

There are several observations to be made from our analysis of the global reaction rate. First, the fits all achieve low variances relative to typical observed concentrations; the solid lines in Figures 3 and 4 illustrate typical fits for our data. On the other hand, our fitted parameters are not in agreement with those of Ref. 6. For example, a large discrepancy exists in predicted values of the methane reaction order parameter. The best fit value from Ref. 6 is 1, while ours are near 2. In addition, our activation energy observed at 275 bar is much greater than that of Ref. 6. The implication is that the

global mechanism from Ref. 6 does not extrapolate to lower temperatures and higher concentrations. Likewise, the best fit for our data will not predict observed data at the conditions of Ref. 6.

Determining the methane reaction order is an important SCWO engineering design issue. If reaction order remained near unity for methane concentrations from 0.001 to 0.1 mole/l, then one could apply the global fit parameters obtained from low-concentration plug-flow experiments to model industrial scale (high-concentration) processes (assuming similar pressures and temperatures). However, our values of reaction order greater than unity indicate that such a model would significantly underpredict rates upstream in the process.

We were interested in knowing if a set of parameters could be found that fits both our data set and that of Ref. 6 taken together. The fact that both fits showed correlations of 0.99 between 'A' and 'E_a' (reported by the fitting routine) means that the true confidence intervals for each set are likely to be much larger than estimated. To explore this possibility, we performed a fit on data sets 1 and 3 (see Table 2) taken simultaneously. Because our high-pressure data set has 219 points while Ref. 6 has 14, each of the latter points were repeated 15 times in this combined fit to give roughly equal weighting to each temperature and concentration range. Each data set's contribution to the total variance of the fit was scaled to account for the two orders of magnitude difference in average methane concentrations. The results from this analysis are shown in the "Combined" column of Table 2. The combined best fit parameters predict the Ref. 6 data with an average error of approximately 5%, and ours within 10%. These results suggest that the simple global model can be used to predict reaction rates over our combined wide range of concentrations and temperatures—useful information for process modeling.

Pressure Dependence of the Methane Reaction Rate

This analysis of the global methane reaction rate describes the dependency of reaction rate on temperature and methane concentration. Our experiments also provide sufficient data to examine the pressure dependency of the reaction. To illustrate the magnitude of this dependency, Fig. 5 presents results from two runs at 400 °C with comparable fuel and oxidizer concentrations, but with different water concentrations. Our data indicate that at our conditions, the oxidation of methane is noticeably faster at the lower total pressures. At 400 °C the effective first-order time constant, τ (the time for methane concentration to fall to its 1/e value), is 65 minutes at 138 bar and 250 minutes at 275 bar. As temperature is raised to 420 °C, τ = 3 minutes at 138 bar and 70 minutes at 275 bar.

We don't have enough information yet to explain these observations. The effect may be chemical and tied to the role of water molecules' participation in key reaction steps. Transport effects could also be responsible if diffusion rates become low enough at the higher pressures so that certain reactions become diffusion-limited. We plan further experiments to investigate these issues—for example, we will conduct the same experiments with argon substituted for water.

Based on published research, this observed increase in methane reaction rate with decreasing pressure is unexpected. Holgate, et al.[11] measured the reaction rates of H_2 and CO with O_2 and found that both increased in rate with total pressure. In that work, an elementary reaction model was developed that successfully predicted many aspects of the reaction kinetics, including the pressure dependence. Schmitt[12] explored the pressure dependence of methanol oxidation using the chemical kinetics code Chemkin Real-Gas[13] and predicted that methanol oxidation rates increase with increasing pressure. Webley used a 66-step model to try to predict methanol[5] and methane[6] oxidation in supercritical water. Webley's results in modeling methanol were in agreement with his experiments, but the same model failed to properly predict methane oxidation rates,[14] yielding predicted rates that were uniformly lower than the observed rates.

We tested the Webley elementary model at conditions representative of our data. Figure 6 shows the results that we obtained using Webley's kinetic model with Chemkin Real-Gas at 400°C and at our two experimental pressures. The model predicts a considerable increase in the reaction rate with increasing pressure. More recent models currently being developed by Butler, Schmitt, and others[15] also predict an increase in rate with pressure. It is important to note that these mechanisms were developed for a particular pressure range not necessarily intended to include total pressures as low as 138 bar.

We also examined the methane reaction order predicted by the Webley mechanism by modeling very lean oxidation (~constant oxygen concentration) at 400 and 600 °C. For this case, the global rate expression is simplified to

$$\text{rate} = d\,[CH_4]/dt = -k\,[CH_4]^a, \qquad (2)$$

where the methane order, 'a,' is determined from the slope of the log(rate) vs. log([CH_4]) plot shown in Figure 7. The resulting curves for both temperatures have slopes (methane reaction orders) that range from 1.4 at low concentrations (0.001 mole/l) to 1.0 at high concentrations (0.2 mole/l). Comparing with Table 2, we see that the Webley model reasonably reproduces the methane dependence of the Ref. 6 data, but fails to predict the methane order of our data.

Conclusion

When fitted to a one-step oxidation mechanism, the low-temperature, high-concentration data obtained in these experiments and the high-temperature, low-concentration data obtained by Webley, et al.[6] produce significantly different global reaction rate parameters. However, because some of these parameters are highly correlated, a single set of four global parameters can be obtained that reasonably fits the combined observations in both sets. No physical significance is attached to each of the resulting parameters since the one-step global mechanism used cannot represent the large number of actual elementary reactions that contribute to the overall rate. On the other hand, the parameters from the combined set can be used to predict methane reaction rates for conditions within the range of these experiments—a useful tool for process modeling.

Our work illustrates some shortcomings of existing elementary models to predict apparent reaction order and pressure trends in methane oxidation. Recent successes elsewhere in predicting H_2 and CO oxidation[11] lend encouragement to our belief that a detailed predictive model can be developed.

The experimental results and analysis presented here reveal several new points about the oxidation of methane by oxygen in supercritical water. Notable are the findings that the apparent reaction order for methane is significantly higher than unity at high concentrations, and that the reaction rate is higher at 138 bar than at 275 bar. In addition, we have shown the utility of *in-situ* spectroscopic monitoring of key reacting species to obtain a large data set of kinetic measurements. In the future, we will be extending this technique to other reacting systems in supercritical water to generate improvements in the predictive capabilities of SCWO process design models.

Acknowledgments

This work was supported by the Department of Defense Strategic Environmental Research and Development Program. The experimental apparatus was developed under funding from the Department of Energy Office of Basic Energy Sciences. We gratefully acknowledge the assistance of Professor Jefferson Tester at Massachusetts Institute of Technology for providing preprints and sharing insights, and the assistance of Professor P. Barry Butler and Robert Schmitt at the University of Iowa for providing current versions of Chemkin Real-Gas, driver codes, and reaction mechanisms. We also acknowledge the efforts of Jason Aiken in conducting the experiments, and the advice of Professor Ian Kennedy at UC-Davis and Donald Hardesty at Sandia.

References

1. Modell M. Processing Methods for the Oxidation of Organics in Supercritical Water. U. S. Patent 4,543,190. September 24, 1985.

2. Thomason T. B., Hong G. T., Swallow K. C., Killilea W. R. The MODAR Supercritical Water Oxidation Process. In: Innovative Hazardous Waste Treatment Technology Series, Freeman H. M., ed. Lancaster, PA: Technomic Publishing Co. 1990: 31.

3. Shanableh A., Gloyna E. F. Subcritical and Supercritical Water Oxidation of Industrial, Excess Activated Sludge. Technical Report CRWR 211. University of Texas at Austin. 1990.

4. Holgate H. R., Webley P. A., Tester J. W., Helling R. K. Carbon Monoxide Oxidation in Supercritical Water: The Effects of Heat Transfer and the Water-Gas Shift Reaction on Observed Kinetics. Energy & Fuels 1992; **6**(5): 586.

5. Webley P. A., Tester J. W. Fundamental Kinetics of Methanol Oxidation in Supercritical Water. In: Johnston K. P., Penninger J. M. L., ed. Supercritical Fluid Science and Technology. Washington, DC: American Chemical Society, 1989: 259.

6. Webley P. A., Tester J. W. Fundamental Kinetics of Methane Oxidation in Supercritical Water. Energy & Fuels 1991; **5**: 411.

7. Thornton T. D., Savage P. E. Kinetics of Phenol Oxidation in Supercritical Water. AIChE Journal 1992; **38**(3): 321.

8. Masten D. A., Foy B. R., Harradine D. M., Dyer R. B. In Situ Raman Spectroscopy of Reactions in Supercritical Water. J. Phys. Chem. 1993; **97**: 8557.

9. Steeper R. R., Rice S. F., Brown M. S., Johnston S. C. Methane and Methanol Diffusion Flames in Supercritical Water. Journal of Supercritical Fluids 1992; **5**(4): 262.

10. Marquardt D. W. An Algorithm for Least-Squares Estimation of Nonlinear Parameters. J. Soc. Ind. Appl. Math. 1963; **11**(2): 431.

11. Holgate H. R., Tester J. W. Oxidation of Hydrogen and Carbon Monoxide in Sub- and Supercritical Water: Reaction Kinetics, Pathways, and Water-Density Effects. J. Phys. Chem. 1993; in press.

12. Schmitt R. G., Butler P. B., Bergan N. E., Pitz W. J., Westbrook C. K. Destruction of Hazardous Waste in Supercritical Water. Part II: A Study of High-Pressure

Methanol Oxidation Kinetics. Fall Meeting of the Western States Section/The Combustion Institute. UCLA: 1991.

13. Bergan N. E., Butler P. B., Dwyer H. A. Chemkin Real-Gas: A Fortran Package for Analysis of Thermodynamics and Chemical Kinetics in High-Pressure Systems. Sandia National Laboratories Technical Report SAND91-8634. 1992.

14. Webley P. A. Fundamental Oxidation Kinetics of Simple Compounds in Supercritical Water. Ph. D Thesis. Massachusetts Institute of Technology, 1989.

15. Butler P. B., Schmitt R. G. Personal Communication. 1994.

Figure Captions

Figure 1. Schematic of the Sandia supercritical water combustor.

Figure 2. Raman spectrum of the ν_1 (symmetric stretch) of CH_4 in supercritical water at 400 °C and 275 bar. Methane concentration is 0.6 mole/l. Integration time was 5 seconds using the 514.5-nm line from a 4-W argon-ion laser.

Figure 3. (a) Experimental data for the oxidation of methane at 400 °C under fuel-lean conditions, and the fit from the global least squares method to all the data at 275 bar. (b) Experimental data for the oxidation of methane at 400 °C under fuel-rich conditions and the fit from the same global least squares method.

Figure 4. Experimental data at 425 °C and equivalence ratio near 1.0, and the fit from the global least squares method to all the data at 275 bar.

Figure 5. Experimental results at 160 and 275 bar for methane oxidation at lean condition at 405 °C with initial concentration of 0.1 mole/l.

Figure 6. Predictions of Chemkin Real-Gas at 400 °C with the kinetic scheme presented in Ref. 6. Note that the model predicts an increase in reaction rate with pressure in contrast to the experimental results shown in Figure 5.

Figure 7. Methane reaction rate as a function of methane concentration predicted by the kinetic scheme in Ref. 6 for very fuel-lean conditions. The slopes of the lines indicate the reaction order of a one-step reaction mechanism with respect to methane concentration.

Table 1 - Summary of Experimental Data

Run #	Temp (°C)	Press (bar)	Total Points	First Methane Conc. (mol/l)	Final Methane Conc. (mol/l)	First Oxygen Conc. (mol/l)	Duration (mins)
1	382	282	16	0.174	0.132	0.182	102
2	382	282	27	0.093	0.052	0.198	214
3	400	277	11	0.243	0.156	0.317	63
4	400	280	12	0.217	0.123	0.282	62
5	400	281	29	0.126	0.053	0.430	194
6	401	276	9	0.211	0.122	0.290	42
7	405	277	12	0.098	0.038	0.851	37
8	405	277	9	0.099	0.059	0.541	27
9	405	278	9	0.259	0.185	0.247	44
10	406	277	13	0.176	0.108	0.273	42
11	425	274	17	0.121	0.033	0.379	99
12	425	277	14	0.116	0.026	0.308	88
13	425	278	16	0.092	0.023	0.400	94
14	441	279	6	0.032	0.018	0.380	30
15	442	280	19	0.064	0.000	0.250	107
16	382	138	15	0.117	0.065	0.335	82
17	402	143	13	0.079	0.022	0.424	67
18	402	143	15	0.066	0.013	0.382	89
19	403	145	13	0.065	0.023	0.650	58
20	403	170	9	0.108	0.003	0.877	39
21	405	139	13	0.090	0.014	0.670	73
22	405	143	9	0.118	0.023	0.622	50
23	405	159	9	0.102	0.021	0.798	44
24	410	139	12	0.090	0.009	0.387	53
25	415	138	14	0.086	0.003	0.396	63
26	420	141	5	0.089	0.011	0.307	19

Table 2 - Results from Fits to the Experimental Data

	#1 This Work 275 bar	#2 This Work 138 bar	#3 Reference 6 243 bar	#1 & #3 Combined
Preexponential Factor, log A	18.7	28.7	11.4	18.6
Activation Energy, Ea (kcal/mole)	60.0	89.9	42.8	60.0
Reaction Order w.r.t. Methane	2.06	1.85	0.99	1.68
Reaction Order w.r.t. Oxygen	0.58	-0.03	0.66	1.02

Figure 1.

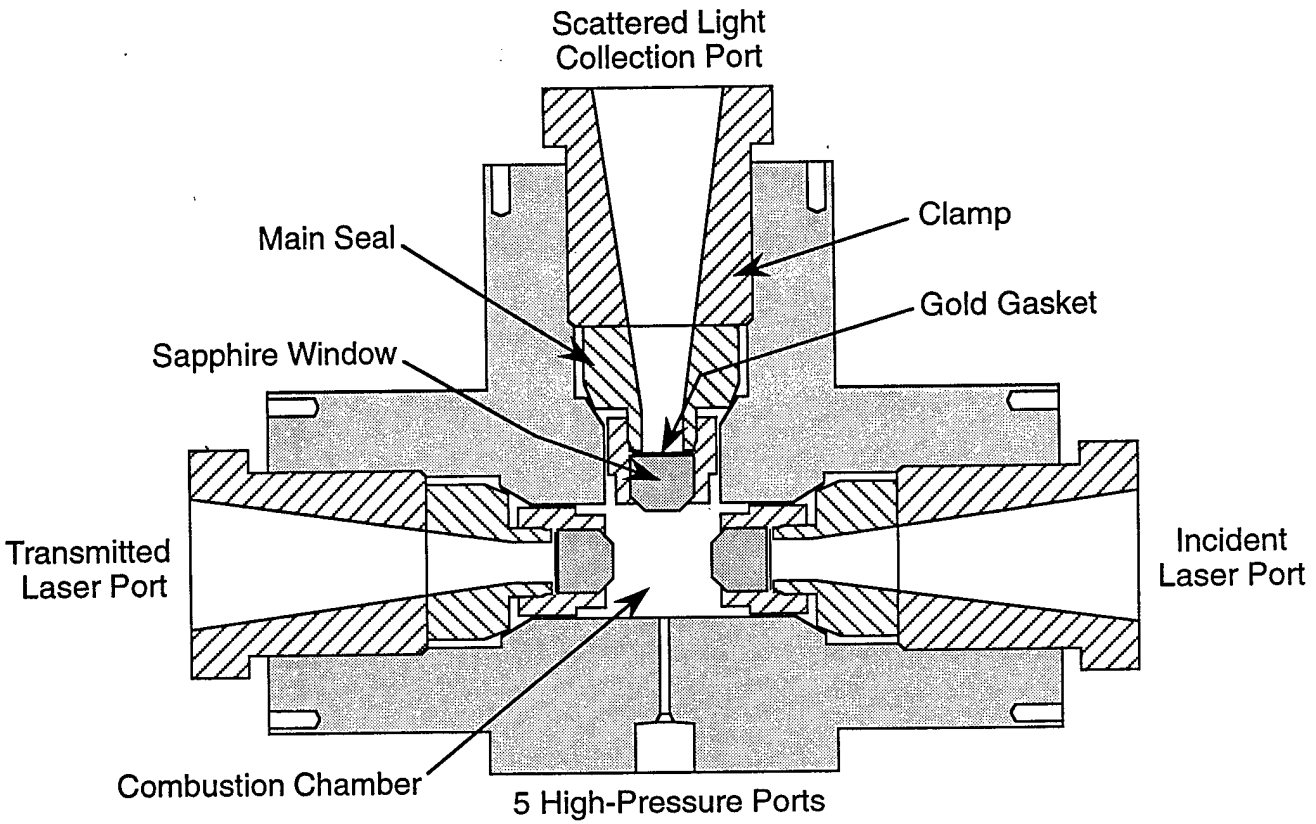
Scattered Light
Collection Port
Clamp
Main Seal
Gold Gasket
Sapphire Window
Transmitted
Laser Port
Incident
Laser Port
Combustion Chamber
5 High-Pressure Ports

Figure 2.

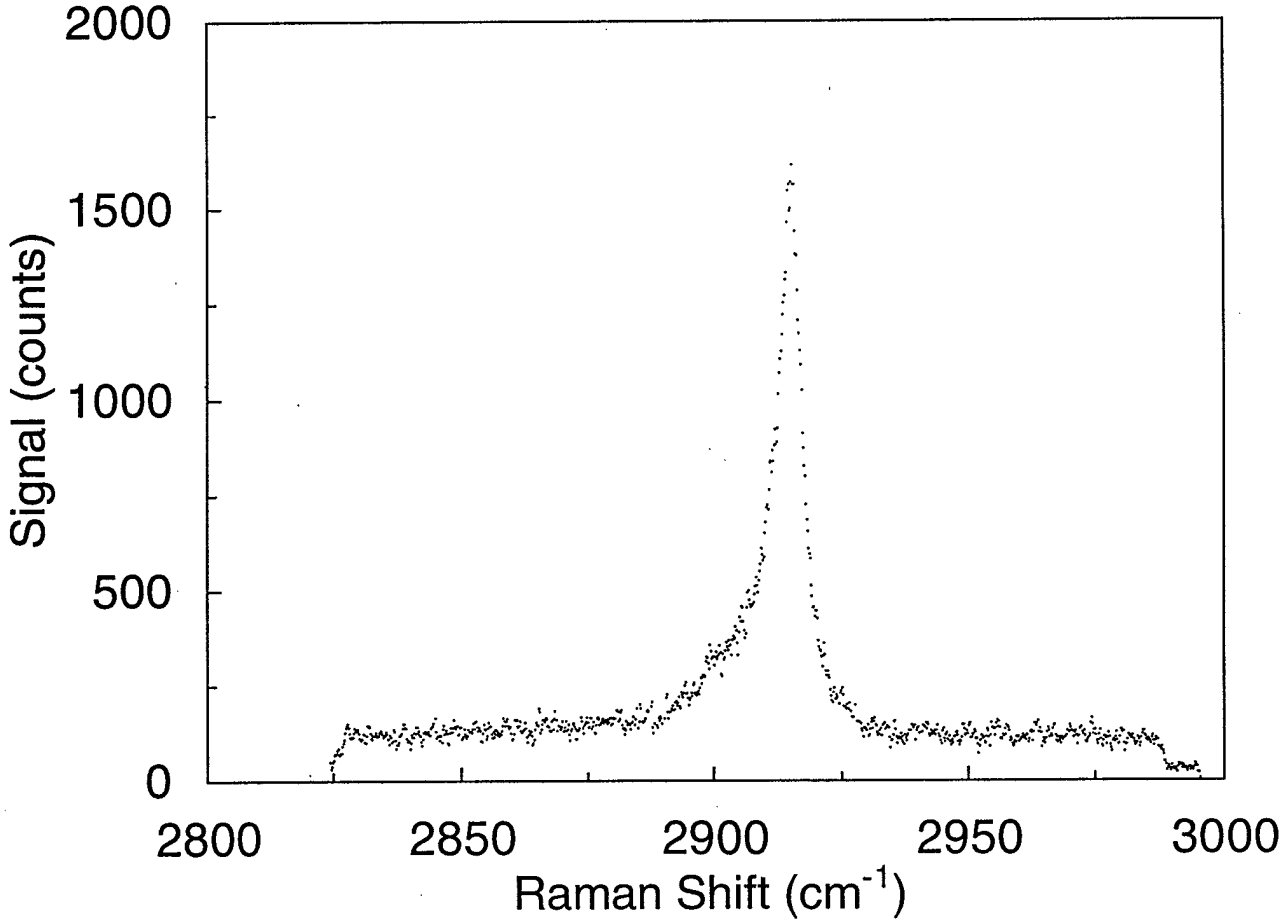
2000
1500
1000
500
0
Signal (counts)
2800
2850
2900
2950
3000
Raman Shift (cm-1)

Figure 3a.

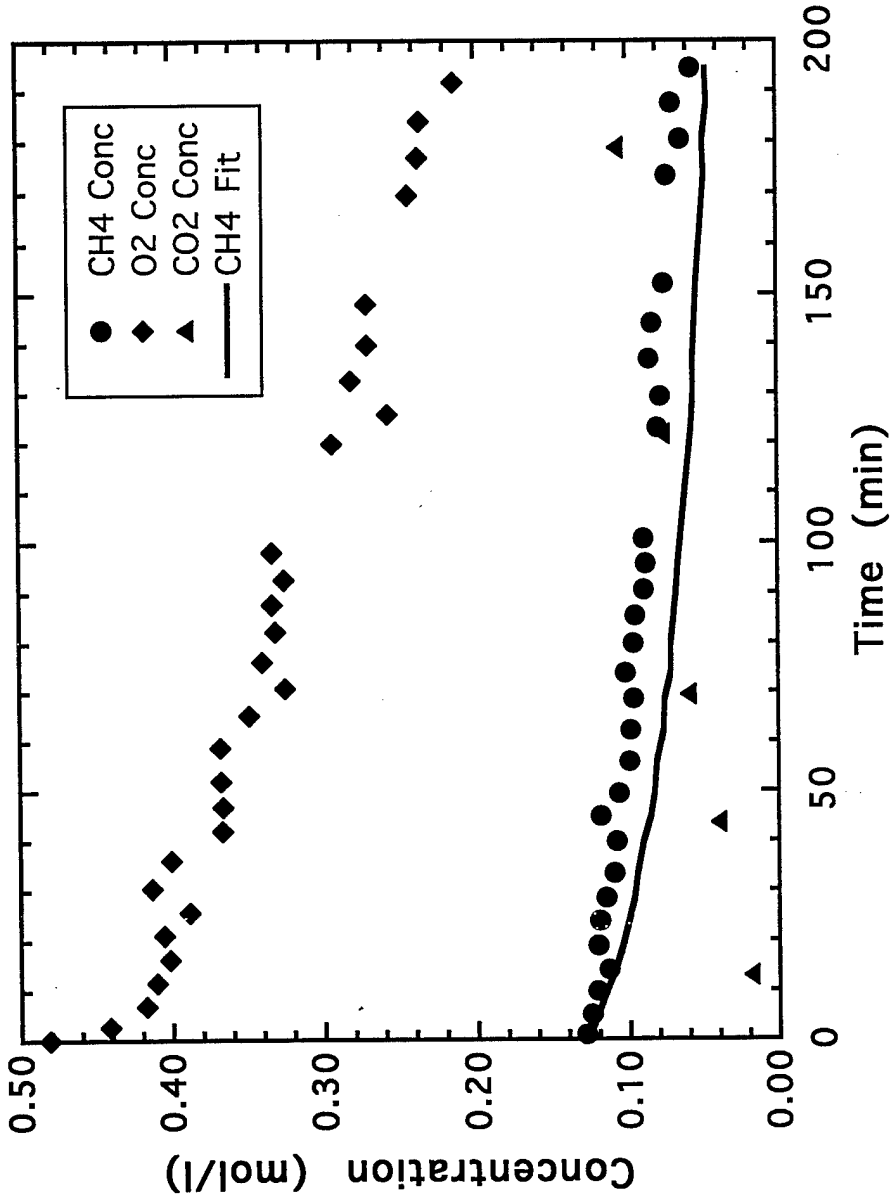
CH4 Conc
O2 Conc
CO2 Conc
CH4 Fit
Concentration (mol/l)
Time (min)
0.00
0.10
0.20
0.30
0.40
0.50
0
50
100
150
200

Figure 3b.

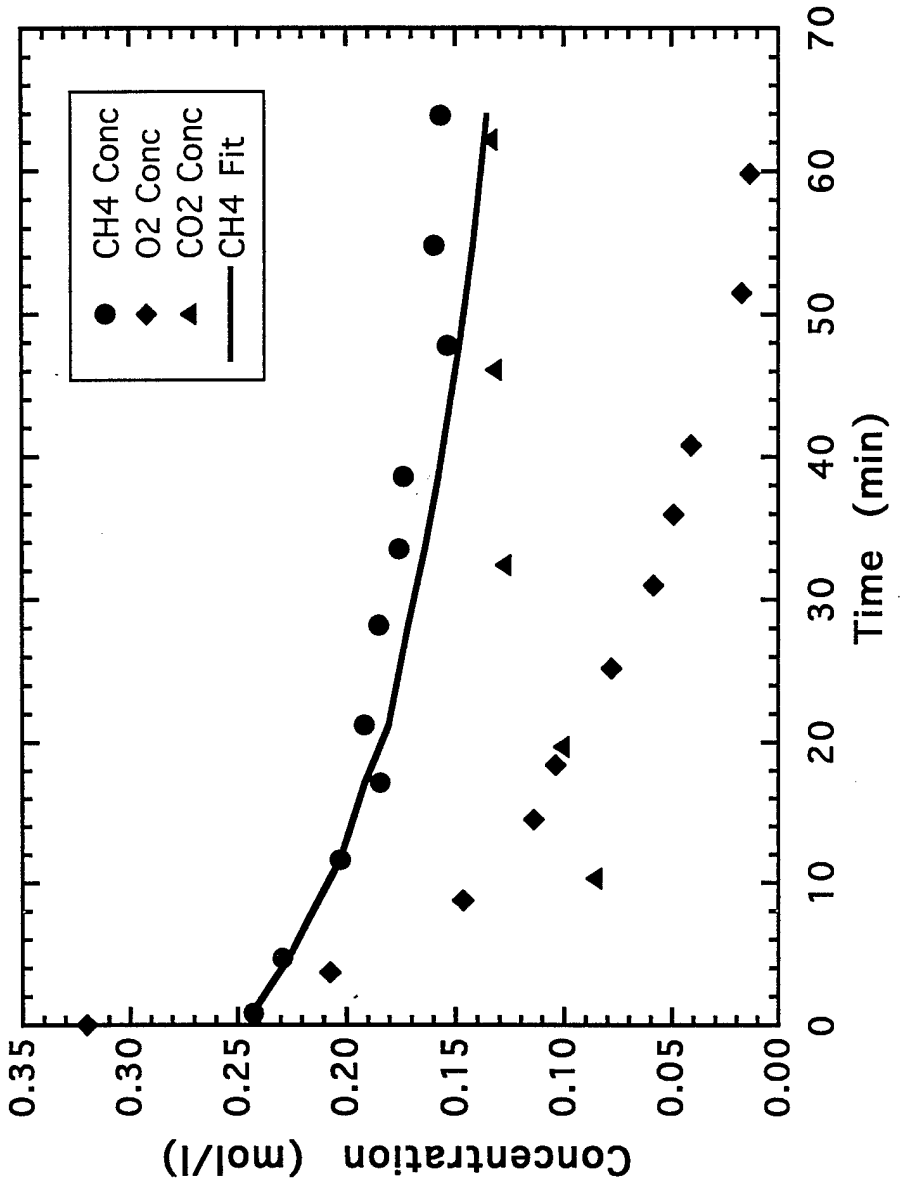
CH4 Conc
O2 Conc
CO2 Conc
CH4 Fit
Concentration (mol/l)
Time (min)
0.35
0.30
0.25
0.20
0.15
0.10
0.05
0.00
0
10
20
30
40
50
60
70

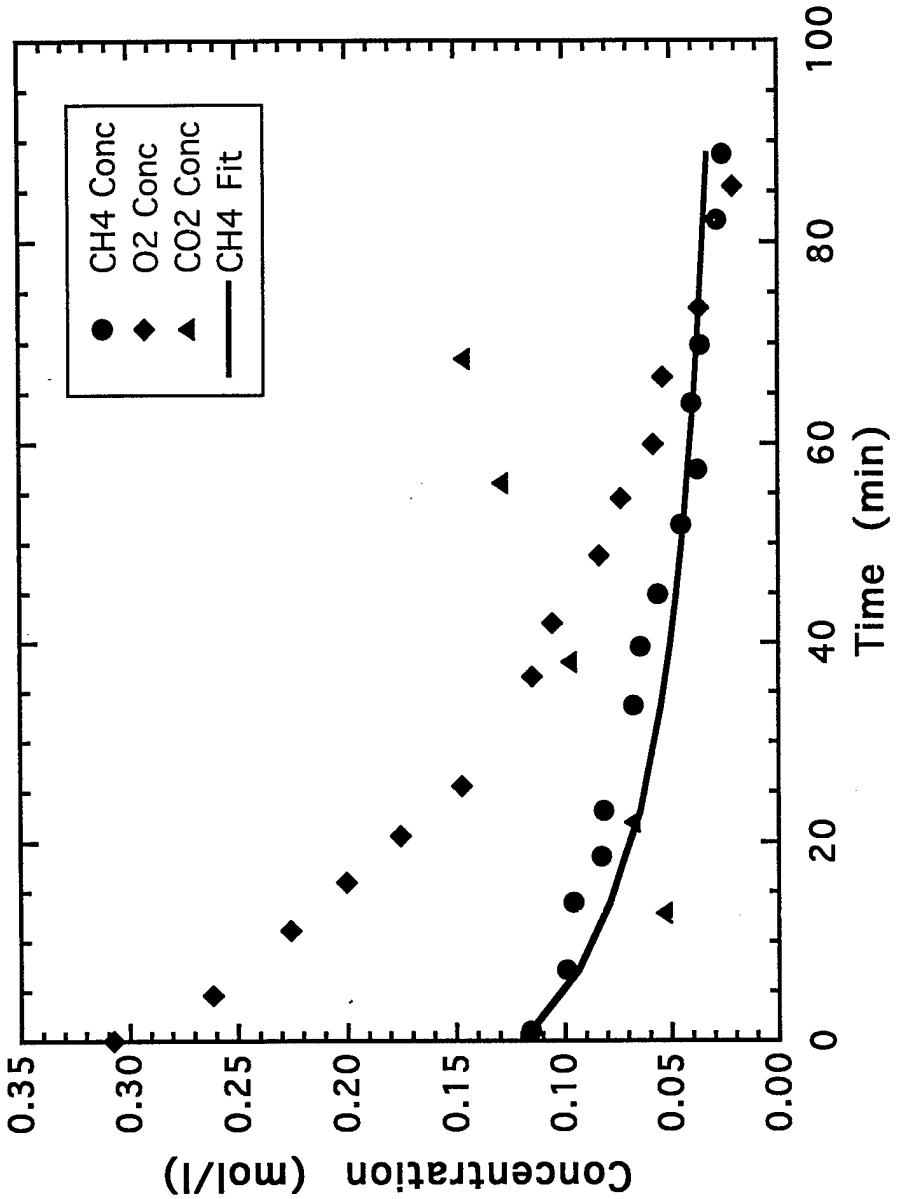
CH4 Conc
O2 Conc
CO2 Conc
CH4 Fit
Concentration (mol/l)
0.35
0.30
0.25
0.20
0.15
0.10
0.05
0.00
0
20
40
60
80
100
Time (min)

Figure 4.

Figure 5.

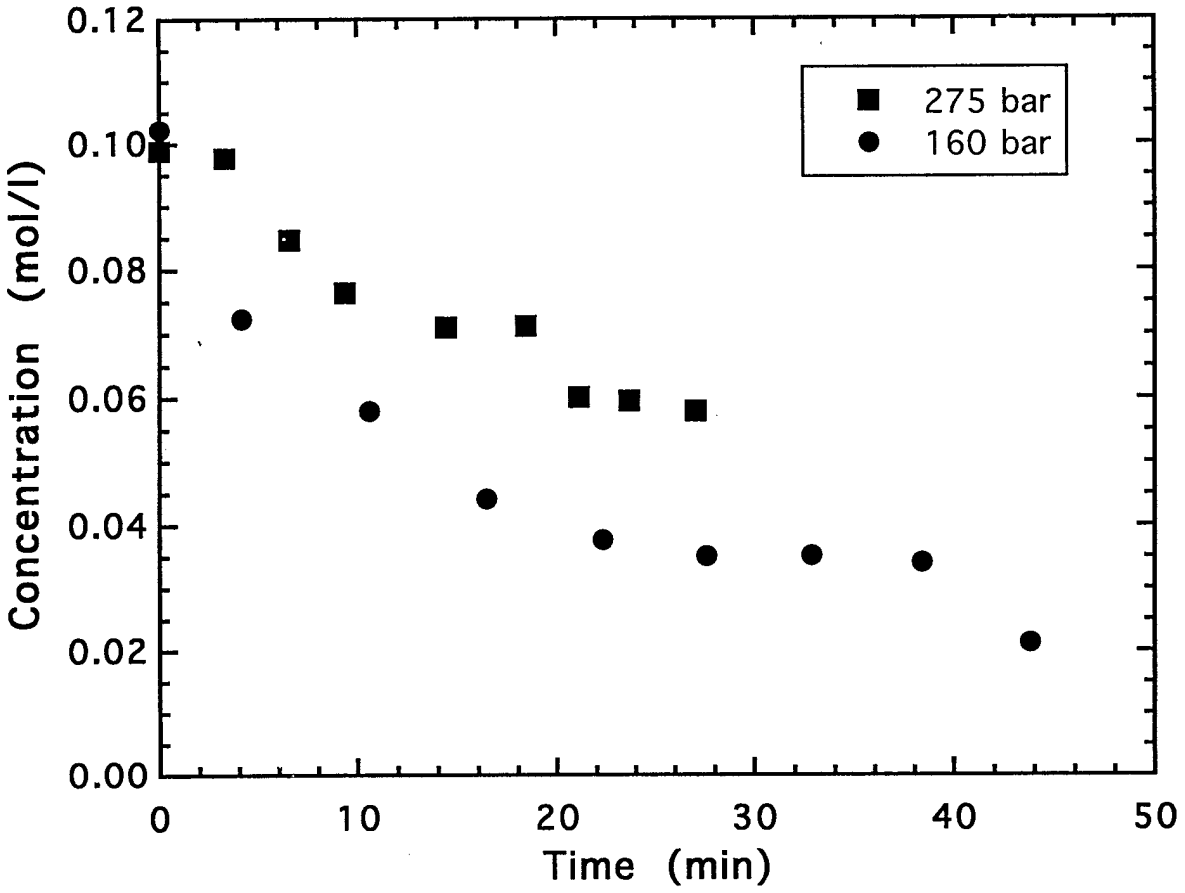
0.12
0.10
0.08
0.06
0.04
0.02
0.00
Concentration (mol/l)
0
10
20
30
40
50
Time (min)
275 bar
160 bar

Figure 6:

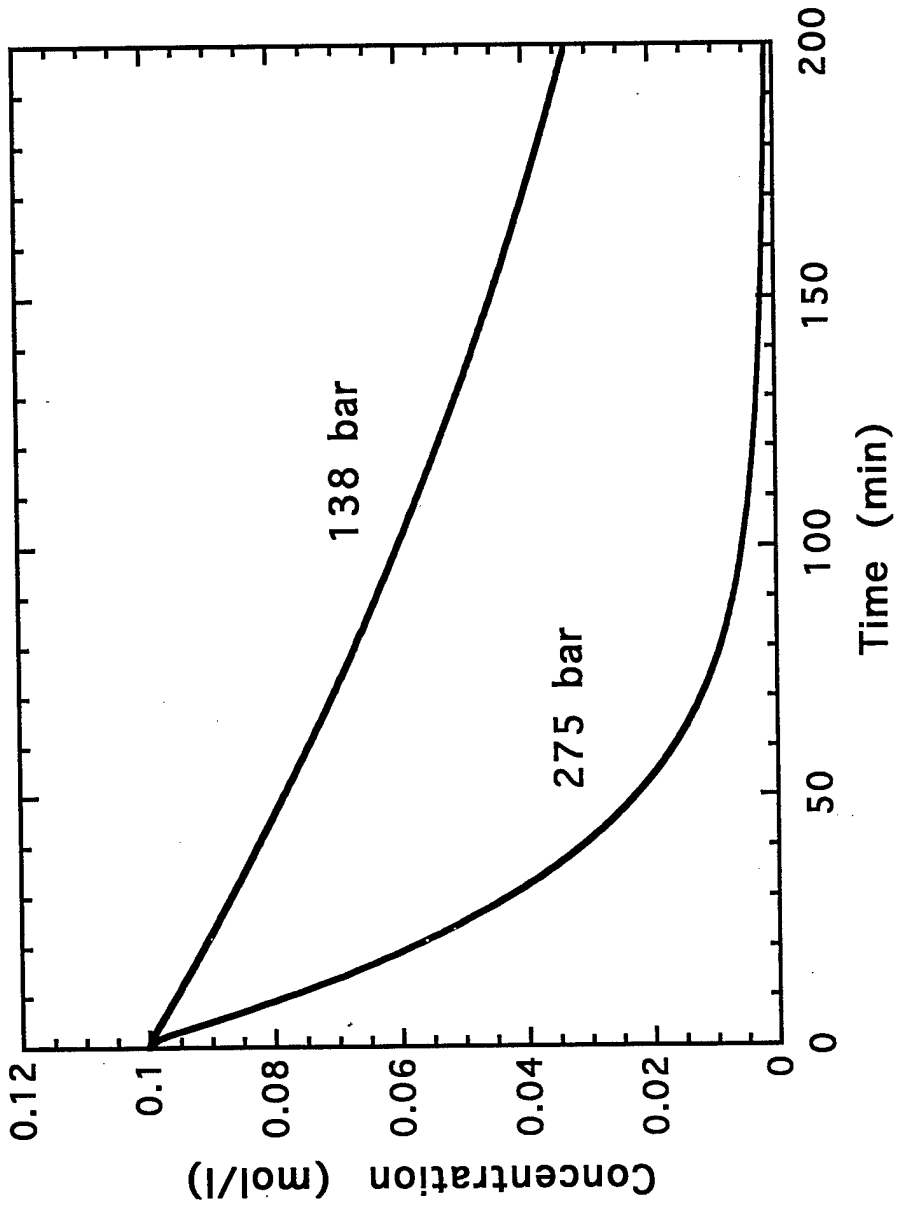
Concentration (mol/l)
0.12
0.1
0.08
0.06
0.04
0.02
0
0
50
100
150
200
Time (min)
138 bar
275 bar

Figure 7.

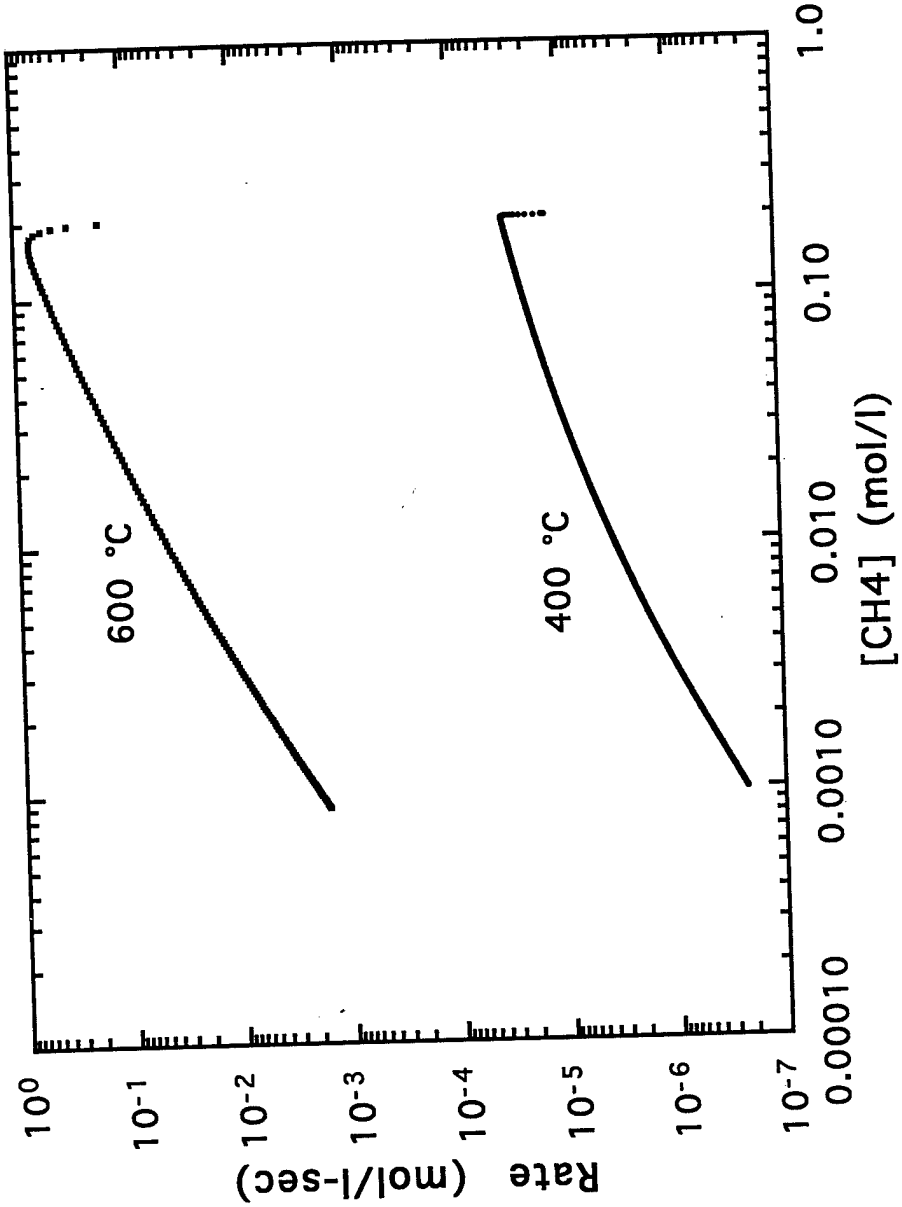
600 °C
400 °C
Rate (mol/l-sec)
[CH4] (mol/l)
10^0
10^-1
10^-2
10^-3
10^-4
10^-5
10^-6
10^-7
0.00010
0.0010
0.010
0.10
1.0